Journal of the European Ceramic Society **18** (1998) 467–477

PII: S0955-2219(97)00168-4
0955-2219/98/$19.00 + 0.00

Influence of Particle Concentration on Rheological Properties of Aqueous α-Al_2O_3 Suspensions

Andreja Zupancic,[a] Romano Lapasin[b]* and Annika Kristoffersson[c]

[a]Faculty of Chemistry and Chemical Technology, University of Ljubljana, Askerceva 5, SI 1001 Ljubljana, Slovenia
[b]Department of Chemical, Environmental and Raw Materials Engineering (DICAMP), University of Trieste, piazzale Europa 1, I 34127 Trieste, Italy
[c]Swedish Ceramic Institute (SCI), Box 5403, S402 29 Göteborg, Sweden

(Received 18 April 1997; accepted 11 August 1997)

Abstract

The influence of particle concentration on the rheological properties of aqueous alumina suspensions is investigated under steady and oscillatory shear conditions. At solid volume fractions between 0·45 and 0·6, a high degree of particle stabilization is achieved when 0·2 wt% of polyacrylic acid is added as a dispersant. With increasing particle concentration the flow behavior changes from pseudoplastic to plastic. The apparent yield stress (from the generalized Casson model) is found to be a significant quantity for characterizing changes in structural conditions of the disperse phase with increasing solids loading even though more detailed information is provided by viscoelastic properties. The analysis of viscoelastic data based on the Friedrich–Braun fractional derivative model and the generalized Maxwell model showed that transitions of particle arrangements due to electrostatic repulsion take place at $\Phi = 0{\cdot}5$ *and 0·55. For these critical concentrations the influence of latex binder addition on the rheological properties is examined.* © *1998 Elsevier Science Limited. All rights reserved*

1 Introduction

Highly concentrated suspensions based on organic solvents represent very important materials in various technological processes, such as the production of paints or ceramics. In recent years, environmental protection and safety reasons have induced the replacement of non-aqueous organic solvents with disperse media based on aqueous chemicals in various industrial fields. Such technological changes occur also in the production of ceramic slips for tape casting, posing a series of problems connected with formulation and processing. Also in the case of aqueous media, an appropriate choice of dispersant type and concentration is compulsory in order to obtain adequate stability of the suspensions and, hence, to ensure acceptable quality of the products. When a solvent based disperse medium is replaced by an aqueous one, the evaporation rate during drying is usually slower. Accordingly, the achievement of the highest possible particle concentration is particularly favorable, because the drying time can be substantially reduced in the process stage following tape casting. High solids loading represents an interesting goal also in other forming methods, such as spray-drying of granules for pressing and in new alternative forming methods.[1–4] At very high solids loading, relatively low viscosity and acceptable elastic response of suspensions can only be achieved in the presence of an optimum dispersion state of particles. This implies the selection of suitable dispersants and binders (if necessary) and good compatibility between the dispersant and the binder.

The increasing trend to use aqueous suspensions of ceramic powders at very high solid loading makes it imperative to study the influence of pH as well as the types and concentrations of dispersants, binders, plasticizers, etc., on the stability of suspensions. Indeed, good criteria for defining the optimum amount of dispersant and/or the proper pH range can only be derived from the knowledge of the rheological behavior of such systems. Even though several experimental investigations have

*To whom correspondence should be addressed.

been carried out on aqueous ceramic suspensions, they are generally restricted to viscosity measurements performed under arbitrary or limited shear conditions or based on simple standard procedures. However, it should be emphasized that colloidal suspensions usually exhibit viscoelastic properties which become more and more significant with increasing particle concentration. Thus, in order to achieve a thorough characterization of the rheological behavior of concentrated ceramic suspensions, the viscoelastic response should be taken into consideration, also because it can provide more detailed information about the structural conditions of the disperse phase in the equilibrium state. In this respect, the knowledge of viscoelastic properties enables one to define the most suitable composition of the suspension more precisely.

The present work is aimed at studying the influence of solids concentration on the rheological properties of aqueous alumina suspensions for tape casting, under both steady and oscillatory shear conditions. The binder and the dispersant selected have been successfully used earlier for tape casting of alumina (product information from Rohm and Haas company).[5,6] A preliminary analysis of the effects produced by dispersant concentration on the rheological properties was performed at different solids contents and, consequently, the optimum amount of dispersant which ensures the highest degree of particle stabilization was chosen for the subsequent series of experimental tests.

We focused our attention mainly on the rheological characterization of alumina suspensions without latex binder, assuming that binder addition would not modify appreciably the rheological properties of the suspensions. This assumption is valid only in the absence of interactions between the dispersant and the binder.[6,7] Otherwise, when such interactions occur or when the binder competes with the dispersant in adsorbing onto the ceramic particle surface, this can result in destabilization of the suspension and lead to inadequate performance of the slip for tape casting and to inferior properties of the final product. A final check of the effect of binder addition was made at two different solids concentrations.

2 Experimental

2.1 Materials and preparation of slurries

A high purity alumina powder AKP 30 from Sumitomo Chemicals was used in this study. According to the manufacturer, the mean particle size, d_{50}, was 0·3–0·4 μm, and the BET specific surface area was 6·8 $m^2\ g^{-1}$. The dispersant and the latex binder added as organic agents (both from Rohm and Haas, USA) had the following characteristics: *dispersant*: Duramax D3021, polyacrylic acid modified with substituted alkyl groups, pH 7, total solids 40%, counterion NH_4, MW 5000; *latex binder*: Duramax B1035, acrylic latex, Tg −40°C anionic surfactant, pH 7·5–8·7, total solids 55%, low viscosity grade, shear thinning. 0·09 Pa s^{-1} at 10 s^{-1}.

Different dispersant concentrations had been considered, ranging from 0·15 to 0·5 wt%, as calculated on the alumina powder, solid dry weight basis. The batch size was in all cases 200 g of alumina. The suspensions at different solid volume fractions, ranging from 0·45 to 0·60, were prepared by ball milling in 0·5 l polypropylene jars filled with 500 g Of Si_3N_4 milling balls for 16 h at a speed of 70 rpm. The pH value of the examined alumina suspensions was 9·3. The rheological measurements of alumina suspensions without binder were carried out 2 h after the preparation.

Alumina suspensions formulated with latex binder were prepared at solid volume fractions of 0·50 and 0·5. The latex binder was added to the alumina suspensions in an amount of 7 wt% of polymer, calculated on alumina powder, and, hence, the polymeric disperse phase corresponded to 22 vol% of total solids content. In this case the dispersant level was 0·2 wt%. The latex binder was added to the alumina suspensions after ball milling and conditioned by magnetic stirring for 2–3 h. The rheological measurements were performed 2 h after the preparation.

2.2 Rheological measurements

Experimental tests were performed at 25 ± 0·1°C, using a rotational rheometer Haake RV20/RC20 with a measuring head CV100 equipped with coaxial cylinder sensor systems ME 30 and ZB 15. A small amount of low viscosity silicone oil, placed above the sample, was necessary to prevent evaporation.

Shear dependent behavior of the examined systems under steady shear conditions was evaluated by ascending and descending shear rate ramps, from 0 to 100 s^{-1} in 5 min, and from 100 to 0 s^{-1} in 5 min, respectively Time dependent properties were checked by applying an on-off stepwise sequence: both steps at constant shear rates (5 and 20 s^{-1} for 3 min) were followed by 5 min no-shear intervals.

The viscoelastic properties of the suspensions were examined under oscillatory shear conditions. In order to determine the limits of linear viscoelastic regime, strain sweep experiments from 0·7 to 10% of strain were carried out at five different constant frequencies (from 0·1 to 2 Hz). The

mechanical spectra of examined suspensions were evaluated by applying frequency sweep experiments in the linear viscoelastic region. The frequency interval explored ranged from 0·05 to 3 Hz at strain amplitudes $\leq 1\%$.

3 Results and Discussion

3.1 Preliminary studies: the influence of dispersant concentration

Optimum stabilization is achieved in ceramic suspensions for tape casting as well as in other suspensions, when the dispersant is adsorbed in a monolayer onto the particle surfaces. Concerning the stabilizing action resulting from the addition of polyacrylic acid as a dispersant, it can be inferred that the particles in examined suspensions were electro-sterically stabilized. According to Cesarano III *et al.*[8] the dissociation of anionic polyelectrolyte increases with increasing pH, and, consequently, the amount of anionic polyelectrolyte which must be adsorbed to achieve the stable suspension decreases. Cesarano and Aksay[9] suggested that more stable and fluid suspensions at high solids concentration could be obtained by optimizing the pH value, so that the corresponding changes in polyectrolyte dissociation and ionic strength lead to more effective electrosteric repulsion between particles. In the case of the suspensions examined, the pH value (around 9·3) enables full dissociation of the used dispersant.

The strong influence of dispersant concentration can be easily deduced from Fig. 1, which reports the values of viscosity at $1\,s^{-1}$ and the storage modulus at 1 Hz for two series of suspensions at solid volume fractions of 0·50 and 0·55, respectively. When the amount of dispersant was lower than the saturation limit of polyelectrolite adsorption on the $A1_2O_3$ particles, the suspensions were unstable and this condition resulted in time-dependent effects for both viscous and elastic quantities. Their values were strongly affected by the previous shear history and increased with increasing shearing time. For both solids loadings the lowest values of the viscosity and the elastic modulus were attained when the dispersant concentration was around 0·2 wt%. A further increase of the dispersant concentration led to an increase in both quantities, with more pronounced effects for the elastic modulus. When the saturation adsorption limit is exceeded, the presence of polymer in the continuous phase gives rise to particle destabilization.[8,9] At dispersant concentrations equal to or above 0·2 wt%, no suspension exhibited any appreciable time-dependent effects. From all these preliminary studies, we selected 0·2 wt% of the dispersant as the optimal concentration to get stable alumina suspensions in the whole solids volume fraction range under examination.

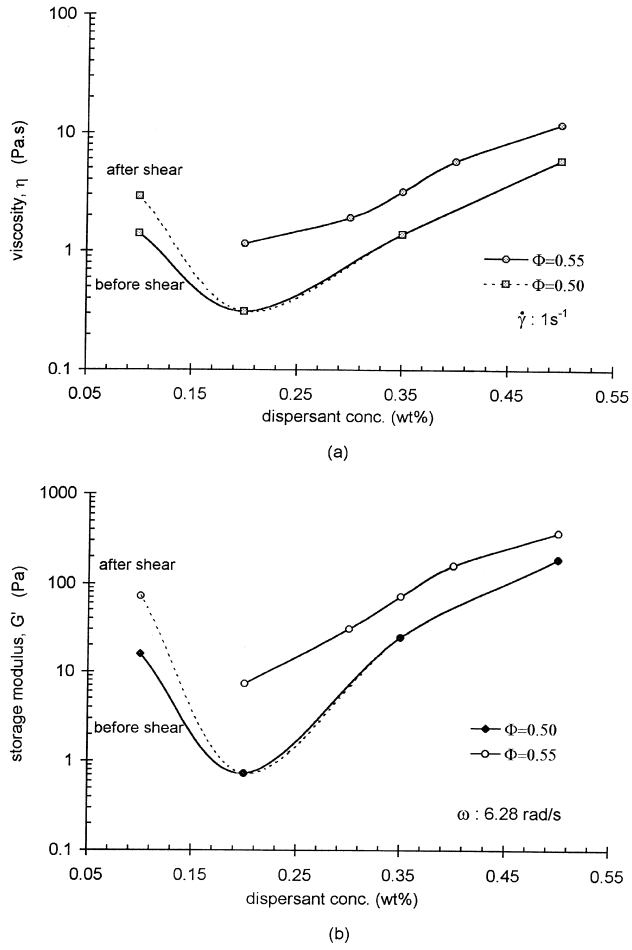

Fig. 1. Influence of dispersant concentration on (a) the viscosity at $\gamma = 1\,s^{-1}$ and (b) storage modulus at $\omega = 6{\cdot}28$ rad s^{-1} for alumina suspensions at $\Phi = 0{\cdot}50$ and 0·55.

3.2 Shear dependent behavior of stable alumina suspensions

In the present work attention is essentially focused on the influence of solid volume fraction on the rheological behavior of well stabilized alumina suspensions. For concentrated suspensions of stable particles, time-dependent effects under continuous shearing conditions are usually negligible and this is also the case with all the alumina suspensions examined. Figure 2 shows that the viscosity values obtained at a constant shear rate do not depend on the shearing time, even at the highest solid volume fraction examined.

Time-dependent effects on the flow behavior are also negligible when the shear rate ramp procedure is carried out. A good superposition of up and down curves is observed in the whole range of particle concentration. From all these experimental evidences relevant to time-dependent effects, we can argue that suspensions exhibit a high degree of

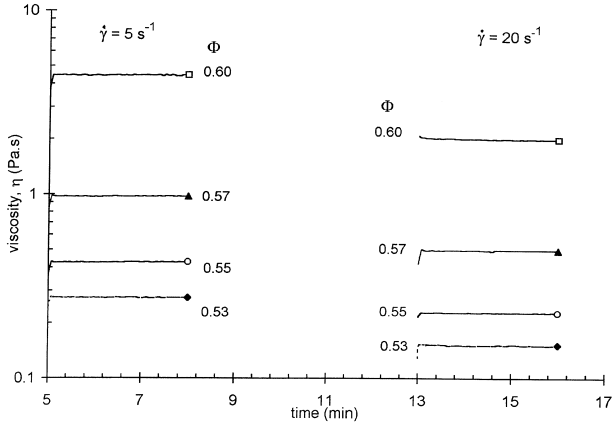

Fig. 2. Time dependent behavior of alumina suspensions ($\Phi = 0{\cdot}53-0{\cdot}60$) at shear rates of 5 and 20 s^{-1}.

particle stabilization; in other words, no appreciable particle aggregation is present.

The influence of particle concentration on shear dependent behavior is illustrated in Fig. 3. Increase in particle concentration leads to the transition from pseudoplastic to plastic flow behavior. Such a transition is usually found also for flocculated suspensions, but at much lower particle concentrations than those examined in this work. The suspensions with solid volume action equal to 0·5 or higher show a tendency to asymptotic increase in viscosity when the shear stress decreases. The occurrence of flow behavior transition at so high solids contents confirms the high stability degree of the systems examined. Among the various rheological models existing in literature, the generalized Casson model gave the best fitting results for describing plastic flow behavior of examined suspensions. The generalized Casson model is:

$$\tau^n = (\tau_y)^n + (\eta_\infty \dot{\gamma})^n \qquad (1)$$

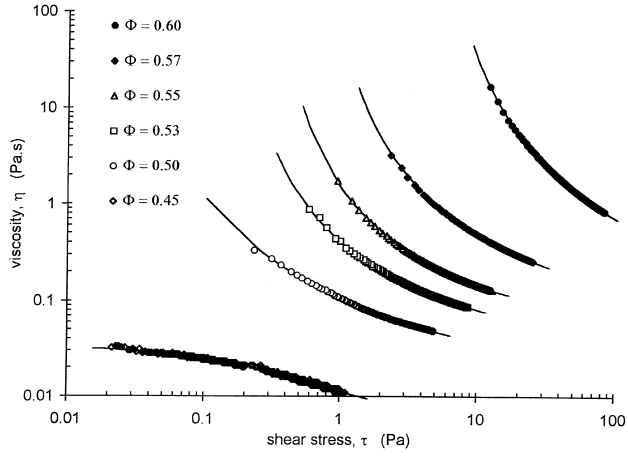

Fig. 3. Flow curves of alumina suspensions at various solid volume fractions ($\Phi = 0{\cdot}45$ —$0{\cdot}60$); solid curves represent correlated values according to eqn (1).

where parameters τ_y and η_∞ represent the yield stress and the limiting viscosity at a high shear rate range. For $n = 0{\cdot}5$ we find the original form of the Casson model. The values of the model parameters are reported in Table 1. For the investigated suspensions, parameters η_∞, and n are not strongly influenced by increased solids loading, since the values of τ_y change appreciably.

The increase in the yield stress with increasing solid volume fraction can be correlated by the following expression:

$$\tau_y = k\left(\frac{\Phi - \Phi_0}{\Phi_m - \Phi}\right)^m \qquad (2)$$

Similar relations can be found in literature, for example Barnes,[10] Wildemuth and Willliams,[11] in fractal approach of Lapasin *et al.*,[12] and for solid volume fraction dependence of compressive yield stress.[13]

Φ_0 represents the lower limit (percolation threshold) of the solid volume fraction at which the disperse phase behaves as a three-dimensional network structure and Φ_m is the maximum packing volume fraction. The influence of solid volume fraction on the apparent yield stress value is shown in Fig. 4, where the solid curve represents the result of data regression according to eqn (2). The following parameters are obtained: $\Phi_0 = 0{\cdot}49$, $\Phi_m = 0{\cdot}62$, $k = 0{\cdot}32$, $m = 1{\cdot}23$.

For suspensions of monomodal non-interactive hard spheres, i.e. in absence of any attractive interparticle interactions, the percolation threshold should be closer to the volume fraction of random particle packing ($\Phi_{rp} = 0{\cdot}64$).[13] The presence of attractive forces between particles leads to the formation of flocs and clusters of flocs and, hence, the percolation limit is drastically shifted to much lower values of solid volume fraction.[14] In the colloidal field, these random tenuous structures produced by particle aggregation are very extended and can consequently be properly treated as fractal objects, because they are self-similar and

Table 1. Parameters of the generalised Casson model for suspensions at various solid volume fractions

Φ (/)	τ_0 (Pa)	η_∞ (Pa s^{-1})	n (/)
0·45[a]			
0·50	0·012	0·010	0·212
0·53	0·127	0·027	0·291
0·55	0·260	0·038	0·299
0·57	0·562	0·052	0·273
0·60	3·437	0·059	0·237
Suspensions with latex binder			
0·50	0·040	0·016	0·295
0·55	0·552	0·054	0·378

[a]$\Phi = 0{\cdot}45$ suspension did not exhibit plastic flow behavior; the behavior was described by using the Cross model.

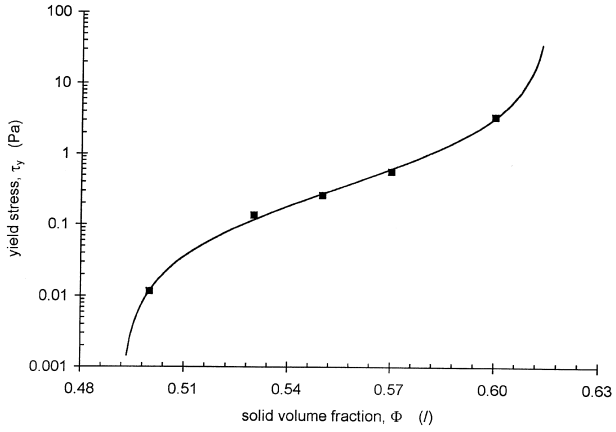

Fig. 4. Dependence of apparent yield stress on solid volume fraction; solid curve is calculated by using eqn (2).

remain invariant under a change of length scale. In such fractal systems, the nature and degree of flocculation rules the density of particle aggregates and determines their fractal dimensionality D. Also when the particles in suspensions are stabilized by long-range electrostatic repulsion, the formation of a three-dimensional network can be expected at solid volume fractions considerably lower than Φ_{rp}.

For the alumina suspensions examined, the percolation limit Φ_0 is 0·49, which is evidently lower than the characteristic random packing for monomodal non-interactive hard spheres. Moreover, it should be noted that the size distribution of the alumina particles used, even though relatively narrow, cannot be considered monomodal. Hence, the maximum packing volume fraction should be slightly higher than 0·64.

The distance between Φ_0 and Φ_{rp} values can be ascribed to the mechanism of particle stabilization, which is essentially based on electrostatic repulsion. The addition of polyacrilyc acid (Mw 5000, gyration radius of 3·2 nm) as a dispersant produces only limited steric effects due to the adsorbed polymer barrier.

If we assume provisionally that the thickness of the adsorbed polymer layer Δ is equal to (or lower than) the gyration radius of polyacrilyc acid under unconstrained conditions, the effective volume occupied by the disperse phase does not differ substantially from the nominal one. At the percolation threshold estimated from the rheological data, the effective volume fraction Φ_{eff} is 0·514 (or less), as can be derived from the following relation:

$$\frac{\Phi_{eff}}{\Phi} = \left(1 + \frac{\Delta}{r}\right)^3 \tag{3}$$

where r is the mean particle radius. At such solids concentration, the alumina particles are not in close contact with one another, since the mean distance S is between 30 and 37 nm; it can be calculated from the following equation:

$$S = 2r\left[\left(\frac{\Phi_{max}}{\Phi_{eff}}\right)^{1/3} - 1\right] \tag{4}$$

where the maximum packing volume fraction Φ_{max} is set to 0·64.

Hence, we can argue that at $\Phi = 0{\cdot}49$, the electrostatic repulsive interactions between charged sites of the polymeric chains adsorbed onto the alumina surface become so significant as to give rise to the formation of a three-dimensional network structure at rest. The particles are constrained in their positions by electrostatic forces and the local stress must exceed a critical value (yield stress) in order to produce a continuous deformation (shear flow) of the particle network. At higher solids concentration ($\Phi > \Phi_0$) the mean distances between particles decrease and, consequently, the increase in repulsive interactions causes a yield stress increase. At $\Phi = 0{\cdot}62$, the effective volume fraction Φ_{eff}, calculated from eqn (3) by setting Δ equal to the polymer gyration radius, almost coincides with the maximum packing value Φ_{rp}. Under such conditions the adsorbed polymeric layers are in close contact with one another and, hence, the particle interlocking prevents the suspension from flowing. Correspondingly, the yield stress goes to an extremely high value ($\tau_y \rightarrow \infty$).

The influence of solid volume fraction on viscosity can be conveniently analyzed in terms of relative viscosity ($\eta_r = \eta$[suspension/η[disperse medium]) and must be referred to one or more reference shear stresses or shear rates, because of the non-Newtonian character of the suspensions. The lower is the selected shear rate or shear stress, the higher are the changes in relative viscosity due to variations of solid volume fraction. Previous studies[15] showed that the shear stress should be the proper reference variable for examining the dependence of relative viscosity on solid volume fraction. Figure 2 demonstrates that for the examined alumina suspensions such analysis can be performed only within a very narrow shear stress range. The dependence of relative viscosity on solid volume fraction at shear stress of 5 Pa is presented in Fig. 5, where the values of suspension viscosity are calculated from the generalized Casson model. The strong concentration dependence of the relative viscosity cannot be described satisfactorily by any of the existing models for $\eta_r(\Phi)$. A possible explanation is that changes in solid volume fraction and shear conditions result in different structural

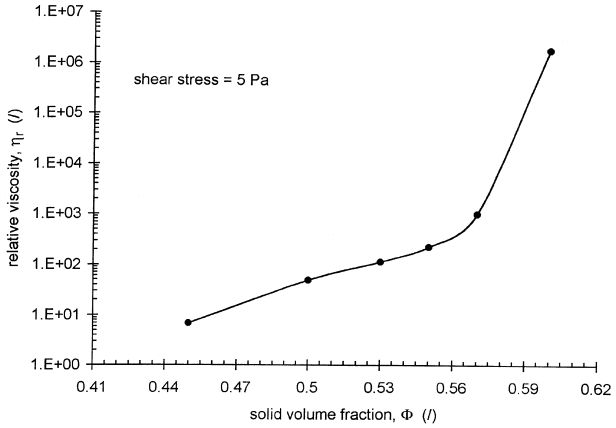

Fig. 5. Influence of solid volume fraction on relative viscosity at reference shear stress of 5 Pa.

arrangements of the disperse phase which are governed by electrostatic particle repulsion.

3.3 Viscoelastic behavior of stable alumina suspensions

The viscoelastic properties of alumina suspensions were examined by dynamic tests. Such experiments must be carried out at a small amplitude of oscillation, so that the test conditions can be considered nondestructive and hence the dynamic functions belong to the linear viscoelastic regime. In the case of concentrated suspensions, the linear viscoelastic region (LVR) is often confined to very low strain amplitudes. The upper limit of strain amplitude above which the viscoelastic properties become nonlinear is usually detected by applying strain sweep experiments at various frequencies. The influence of strain amplitude on the complex modulus G^* and the phase lag δ for suspensions at $\Phi = 0{\cdot}57$ and 0·60 is illustrated in Fig. 6. A first inspection of the profiles of both quantities clearly indicates that the upper limit of LVR lies at shear strains between 1 and 2%. Similar variations of G^* and δ with increasing strain amplitude were obtained for all the suspensions examined. The data evaluated from the strain sweep experiment have been treated by the following expressions, which are similar to the damping functions frequently used for describing non-linear viscoelastic response:

$$G^* = G_0^* \frac{1 + b\gamma^p}{1 + a\gamma^p} \tag{5}$$

$$\delta = \delta_0 \frac{1 + g\gamma^q}{1 + h\gamma^q} \tag{6}$$

G_0^* and δ_0 represent the values of the complex modulus and the phase lag in the linear viscoelastic regime, respectively. The critical strain amplitude γ_c, which marks the upper limit of the linear viscoelastic region, is arbitrarily derived from the following criterion: $\gamma = \gamma_c$ when $G = 0{\cdot}95G_0^*$. The values of G_0^*, δ_0 and γ_c obtained for the suspensions at different solid volume fractions from strain sweep data at 1 Hz are reported in Table 2. The strain sweep experiments performed at different frequencies served to verify the influence of applied frequency on the limits of LVR and to collect preliminary data about the mechanical spectra of examined suspensions. These tests showed that the upper LVR limit does not vary appreciably with decreasing frequency, since γ_c values still lie in the range 1·5–3%. In conclusion, the frequency dependence of dynamic functions under linear viscoelastic conditions can be obtained for all examined suspensions by carrying out frequency sweep tests at strain amplitudes lower than 1%. Figure 7 illustrates the influence of particle concentration on the frequency dependence of the storage modulus (G') and the loss modulus (G''). In the frequency range examined, both moduli increase with increasing solid volume fraction and the viscoelastic response of the alumina suspension progressively changes from more viscous to more

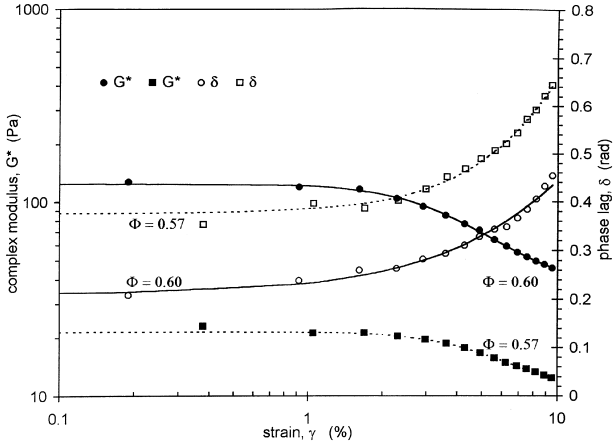

Fig. 6. Determination of the upper limit of LVR for suspensions at $\Phi = 0{\cdot}57$ and 0·60 from strain sweep experiments; solid curves represent correlated values according to eqns (5) and (6).

Table 2. Critical strain amplitude which determines the upper limit of LVR and the corresponding values of complex modulus (G^*) and phase lag (δ) evaluated from eqn (5) at frequency of 6·28 rad s^{-1}.

Φ(/)	γ_C (%)	G_0^* (Pa)	δ (rad)
0·45	5·34	0·415	1·30
0·50	2·52	1·662	1·10
0·53	1·28	5·382	0·731
0·55	2·26	9·022	0·572
0·57	2·40	21·40	0·377
0·60	1·28	124·02	0·212

elastic. At the lowest particle concentration ($\Phi = 0{\cdot}45$) the behavior is essentially viscous in nature ($G' < G''$) in the whole frequency window explored, while a crossover of the curves $G'(\omega)$ and $G''(\omega)$ appears at $\Phi = 0{\cdot}53$ and, finally, at the highest particle concentration ($\Phi = 0{\cdot}60$) the elastic contribution exceeds the viscous one ($G' > G''$) over the entire ω range, as illustrated in Fig. 7(a). When the solid volume fraction increases, more noticeable changes are observed for the elastic component [Fig. 7(b)]. At lower solid volume fractions both moduli continuously increase with increasing frequency, with stronger variations for the storage modulus. With increasing solid volume fraction the traces of $G'(\omega)$ and $G''(\omega)$ are more and more close and similar and become parallel to each other at a solid volume fraction around 0·55. The conditions correspond to an apparent sol–gel transition according to the criterion suggested by Winter and Chambon.[16,17] A further increase in particle concentration reduces the influence of frequency on G' and G''.

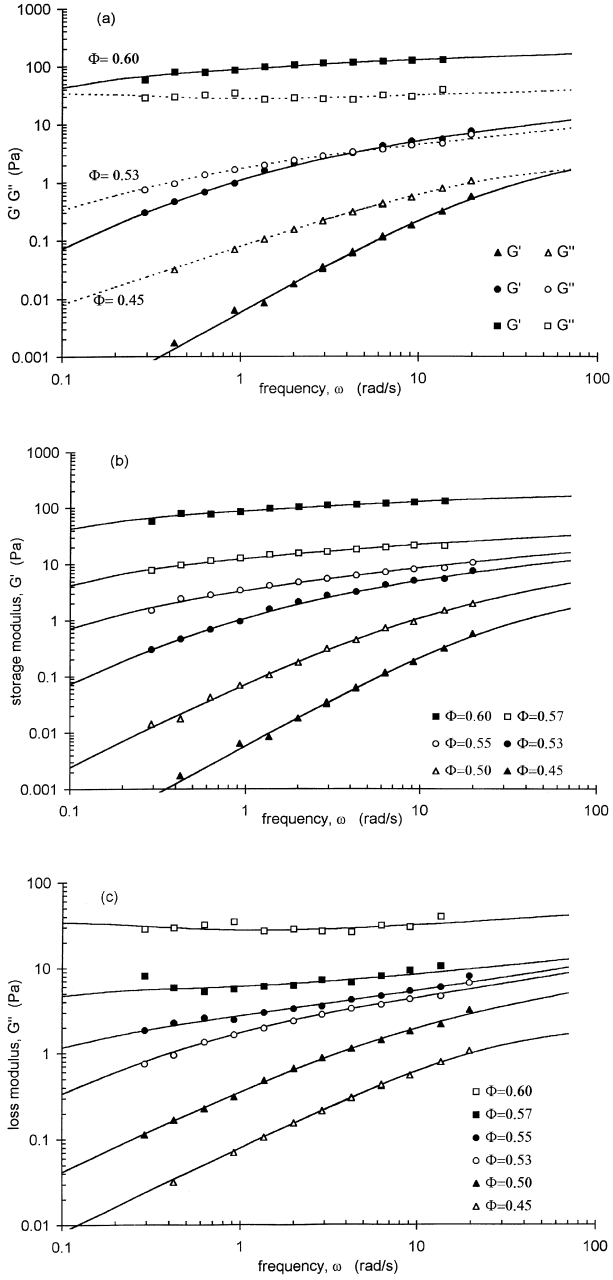

Fig. 7. (a) Frequency dependence of storage and loss moduli for suspensions at $\Phi = 0{\cdot}4$, 5 0·53 and 0·57, influence of particle concentration on frequency dependence of (b) storage modulus and (c) loss modulus. Solid curves represent correlated values by applying eqns (8) and (9).

Stable colloidal concentrated suspensions generally exhibit strong elastic responses when the average distance between particles equals the length scale of the repulsive interparticle interactions. In other words, the viscoelastic properties of such stable systems originate from the repulsive interparticle potential.[13]

The frequency dependence of both dynamic moduli can be described with satisfactory approximation by the model suggested by Friedrich and Braun,[18] belonging to the class of fractional derivative models. This model was selected because it can describe a wide range of viscoelastic responses, from pure viscous liquids to elastic solids, by a limited number of parameters. In the differential form the model can be expressed as:

$$\bar{\bar{\tau}} + D^c[\bar{\bar{\tau}}] = G_\infty\{\mathrm{D}^0[\bar{\bar{\gamma}}] + D^c[\bar{\bar{\gamma}}]\} + \Delta G D^d[\bar{\bar{\gamma}}] \quad (7)$$

where $\bar{\bar{\tau}}$ and $\bar{\bar{\gamma}}$ are the stress and strain tensors, respectively, and c and d are the derivation orders. When $c = d = 1$, the equation corresponds to the 'solid model' for $G_\infty > 0$, whereas the canonical Maxwell 'liquid model' is obtained for $G_\infty = 0$. Equation (7) leads to the following relations for the mechanical spectra:

$$G'(\omega) = G_\infty + \Delta G \frac{(\lambda\omega)^d\left[\cos\left(d\frac{\pi}{2}\right) + (\lambda\omega)^c\cos\left((d-c)\frac{\pi}{2}\right)\right]}{1 + 2(\lambda\omega)^c\cos\left(c\frac{\pi}{2}\right) + (\lambda\omega)^{2c}} \quad (8)$$

$$G''(\omega) = \Delta G \frac{(\lambda\omega)^d\left[\sin\left(d\frac{\pi}{2}\right) + (\lambda\omega)^c\sin\left((d-c)\frac{\pi}{2}\right)\right]}{1 + 2(\lambda\omega)^c\cos\left(c\frac{\pi}{2}\right) + (\lambda\omega)^{2c}} \quad (9)$$

G_∞ represents the equilibrium modulus when the frequency tends to zero and, hence, the model describes liquid-like responses if $G_\infty = 0$. Parameter λ_0 is the characteristic time of a material, which determines the role of the relative contribution of elastic and viscous components in the viscoelastic response and, consequently, the extension of the frequency region where the elastic or viscous contribution prevails. When $c = d = 1$ and $G_\infty = 0$, λ_0 becomes the relaxation time of the Maxwell model. Hence, λ_0 can be referred to as the

fractional relaxation time. The Friedrich and Braun model generalizes the relation proposed by Tschoegl (1989) for the relaxance of the Cole–Cole behavior by introducing an additional parameter (exponent d). The exponent c in eqn (8) and eqn (9) originally comes from Cole–Cole functions When $d = 1$, the decrease in the exponent c ($c \leq 1$) affects the shape of the curve $G'(\omega)$ over the whole frequency range, whereas the material function $G''(\omega)$ is appreciably modified only at higher frequencies. This results in the appearance of asymmetry of $G''(\omega)$ which is often observed for various real materials and cannot be described by the original form of Cole–Cole behavior.

Apparently, the model provides an adequate correlation of loss and storage moduli as the function of frequency in the whole concentration range. Figure 7(a)–(c) reports a comparison between experimental data and solid curves calculated from eqns (8) and (9). In order to obtain reasonable values of the parameters in eqns (7) and (8), the yielding conditions $0 < c < d < 1$ and $G_\infty \geq 0$ should be satisfied. As an objective function in the minimization procedure, the mean squared relative deviation was used. Evaluation of the model parameters by applying the fitting procedure simultaneously for both $G'(\omega)$ and $G''(\omega)$ showed that for the studied suspensions exponent d and parameter G_∞ converged to the limiting conditions $d = 1$ and $G_\infty = 0$. Consequently, the influence of solid volume fraction on the frequency dependence of the dynamic moduli is described through the variation of only three parameters: ΔG, λ_0 and c, as illustrated in Fig. 8.

Although most suspensions do not have a single but rather a range of relaxation times, it is well known that the relaxation time increases with increase in the solid volume fraction. In the range of lower particle concentrations examined, the increase in solid volume fraction results in an appreciable increase in the fractional relaxation time (λ), whereas ΔG and c do not vary significantly. Above 0·55, further increase in solid volume fraction leads to a pronounced increase in both parameters ΔG and c, whereas λ_0 reaches a plateau region. The variations of parameters of the fractional derivative model clearly show that the transition of the viscoelastic response emerges at solid volume fractions around 0·55.

The crossing of the curves $G'(\omega)$ and $G''(\omega)$ generally corresponds to the reciprocal relaxation time of the material and can be explicitly determined from eqns (8) and (9):

$$(\lambda_0\omega)^c = \frac{\sin\left(d\frac{\pi}{2}\right) - \cos\left(d\frac{\pi}{2}\right)}{\cos\left((c-d)\frac{\pi}{2}\right) - \sin\left((c-d)\frac{\pi}{2}\right)} \qquad (10)$$

Variations in the crossing frequency and the corresponding reciprocal relaxation time with increasing solid volume fraction are shown in Fig. 9. The net transition occurring for both parameters between Φ values around 0·50 and 0·55 clearly indicate the existence of two critical conditions, related to microstructural changes.

In order to check the influence of particle concentration on the mechanical spectra, to obtain a more detailed overview of changes in the suspension microstructure and, finally, to confront the fractional derivative approach suggested by Friedrich and Braun with another (more conventional) description of viscoelastic properties, we can extend the analysis by fitting experimental data with the well-known generalized Maxwell model. Under oscillatory shear conditions, the linear viscoelastic response is expressed through the following equations:

$$G'(\omega) = \sum_i \frac{g_i \lambda_i^2 \omega^2}{\left(1 + \lambda_i^2 \omega^2\right)} \qquad (11)$$

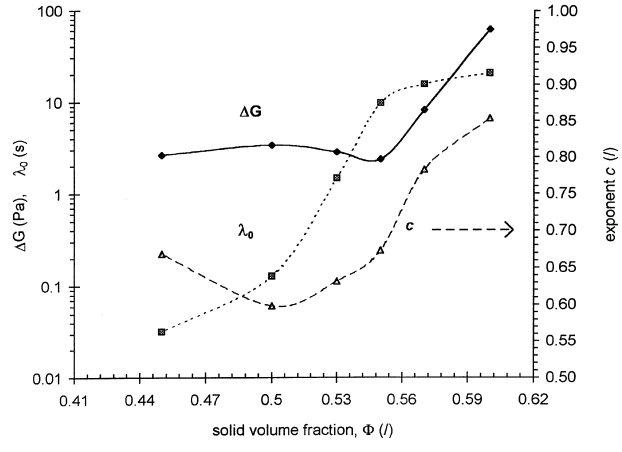

Fig. 8. Influence of solid volume fraction on the variation of parameters ΔG, λ_0 and c in eqns (8) and (9).

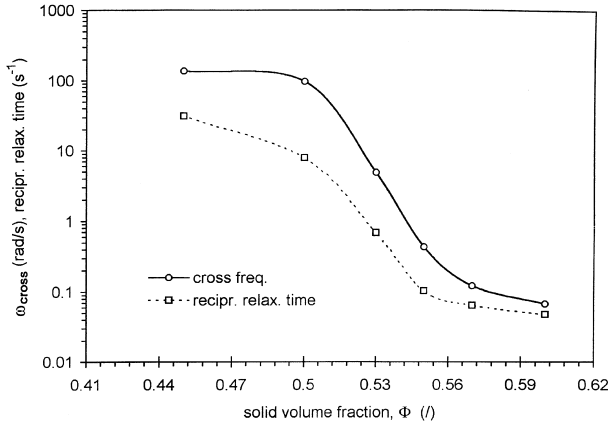

Fig. 9. Influence of solid volume fraction on the variation of crossing frequency and reciprocal relaxation time correlated by using eqn (9).

$$G''(\omega) = \sum_{i} \frac{g_i \lambda_i \omega}{\left(1 + \lambda_i^2 \omega^2\right)} \qquad (12)$$

where λ_i and g_i represent the relaxation time and the elastic modulus of the ith Maxwell element. To avoid problems concerning the evaluation of fitting parameters λ_i, g_i from the experimental data, it is necessary to fix a maximum number of elements and to set a constraint which only allows positive values of parameters g_i. Application of eqns (11) and (12) showed that the viscoelastic responses of all suspensions examined can be satisfactorily described with a series of four Maxwell elements in parallel. The results of this approach, i.e. the relaxation spectra $g_i(\lambda_i)$, are illustrated graphically in Fig. 10.

Increase in solid volume fraction gives rise to a transition of the relaxation spectrum which changes from edge-type to box-type at $\Phi = 0{\cdot}5$. For suspensions at lower particle concentrations the coefficients g_i monotonically decrease with increasing relaxation time λ_i (edge-type distribution) which is often found for non-structured systems. At higher solid volume fractions ($\Phi \geq 0{\cdot}55$) the variation of the coefficients g_i with increasing λ_i is not monotonic and a box-type contribution appears at longer relaxation times, which is typical for structured materials. A slightly higher quality of data fitting is provided by eqns (11) and (12) because of a higher number of adjustable parameters. Another motive for resorting to the generalized Maxwell model to describe mechanical spectra of the alumina suspension was that the viscoelastic behavior of the suspension composed of alumina and latex binder with the highest solids content could not be described adequately by eqns (8) and (9).

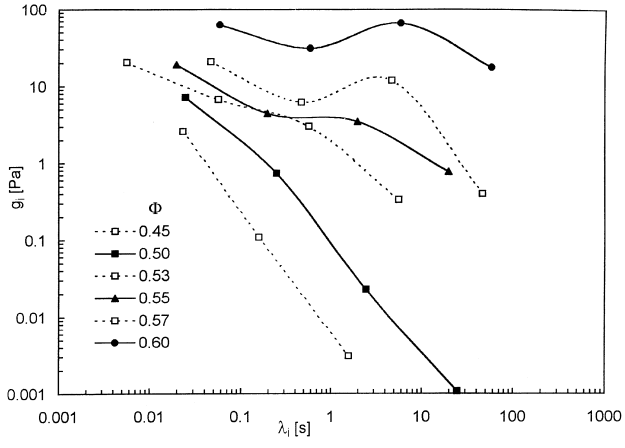

Fig. 10. Spectrum coefficient evaluated by using eqns (10) and (11) for suspensions at various solid volume fractions. $\Phi = 0{\cdot}45 - 0{\cdot}60$.

3.4 Effects of binder addition

Suspensions at solid volume fraction of 0·50 and 0·55 were selected as reference systems for the final check of the influence of latex binder on the rheological properties. The examination of alumina suspensions without latex binder indicated that at these two solid volume fractions significant transitions of rheological behavior can be expected. As we mentioned in the introduction, the binder addition cannot modify appreciably the rheological properties of suspensions if the interactions between the dispersant and the binder are negligible. When the experiments were performed under steady shear conditions, the flow curves of the corresponding systems (without and with the binder, respectively) converge at high shear rates (Fig. 11). Detectable effects on shear viscosity were observed only in the low shear stress range and, consequently, higher yield stress values were evaluated from the Casson model (Table 1). The viscosity increase produced by binder addition was more pronounced at $\Phi = 0{\cdot}55$. All these considerations lead to the conclusion that a preliminary study of alumina slips can be considered a satisfactory reference basis for predicting the shear behavior of tape casting slurries, at least in a first-order approximation.

More remarkable effects of the addition of latex binder are observed for viscoelastic properties as can be observed in Fig. 12. The solid curves in Fig. 12 represent calculated values of G' and G'' according to eqns (11) and (12), respectively. The suspensions containing latex binder display higher values of both moduli, and appreciable differences are observed for elastic contribution. In this case also a more noticeable increase in both moduli appears at the low frequency range. This can be essentially ascribed to a shift of the relaxation spectrum towards longer relaxation times. The spectrum coefficients γ_i and g_i for the suspensions formulated with and without latex binder are

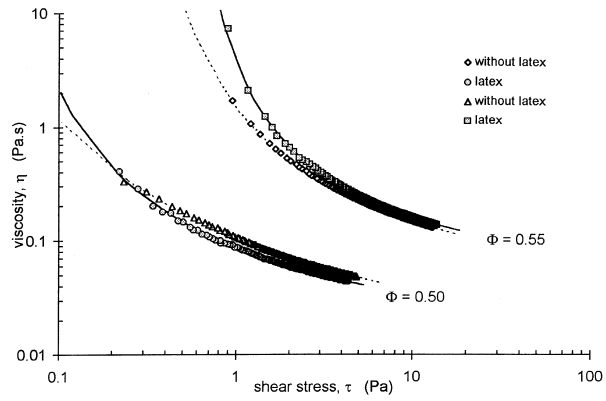

Fig. 11. Flow curves of suspensions with and without latex binder; solid curves represent correlated values according to eqn (1).

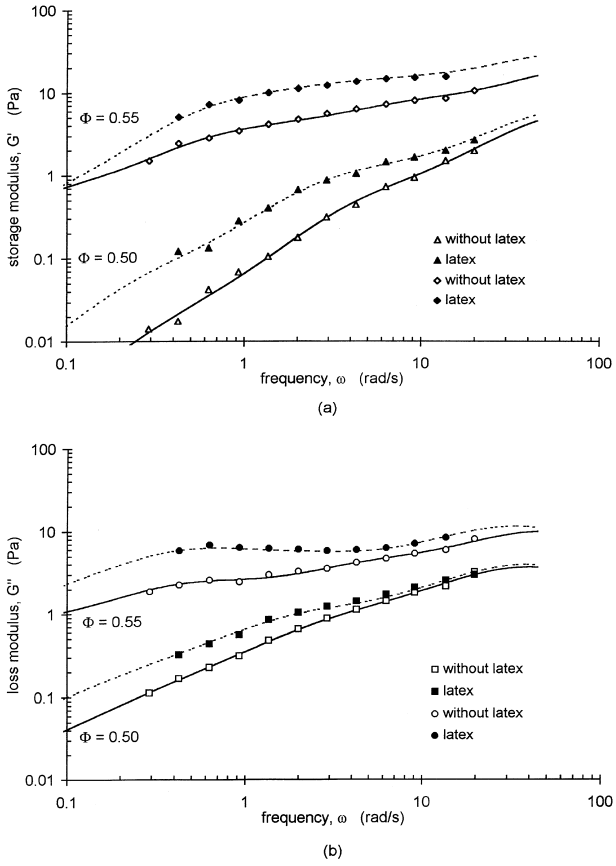

Fig. 12. Frequency dependence of (a) G″ and (b) G′ for suspensions at $\Phi = 0{\cdot}50$ and 0·55 composed with and without latex binder.

compared in Fig. 13. At a lower particle concentration ($\Phi = 0{\cdot}50$) binder addition displaces the set of relaxation times towards higher values, whereas at a higher particle concentration ($\Phi = 0{\cdot}55$) the profile of the relaxation spectrum changes and becomes similar to that obtained for the suspension at $\Phi = 0{\cdot}7$ without binder addition. From such examination of viscoelastic properties we can infer that the presence of latex binder in

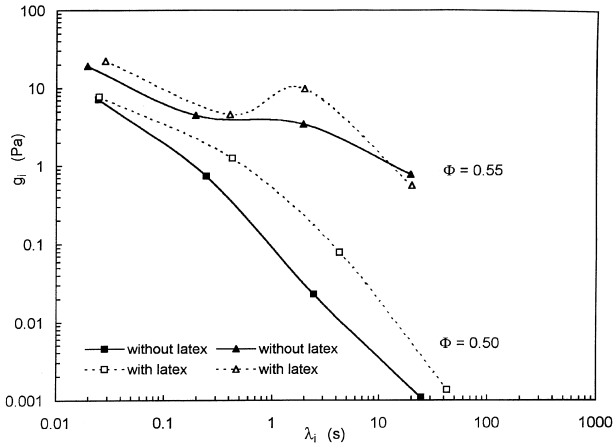

Fig. 13. Influence of added latex binder on the evaluated spectrum coefficients [(eqns (10) and (11)] for suspensions at $\Phi = 0{\cdot}50$ and 0·55.

the disperse phase may affect the microstructure of electrosterically stabilized alumina particles. More pronounced effects are to be expected at higher particle concentrations, where the electrostatic repulsive interactions become significant. In the case of examined suspensions the addition of latex binder results in an increase in repulsive particle interactions, which leads to a tighter particle network structure at rest. Moreover, we observed that steady shear viscosity data are similar for suspensions with and without the binder and at the same solid volume fraction, so it can be argued that the presence of binder does not give rise to any appreciable destabilization of the suspension.

4 Conclusions

Rheological examination of the investigated aqueous alumina suspensions (pH 9·3) showed that the optimal dispersant quantity is around 0·2 wt%. At this concentration, the saturation adsorption limit of fully dissociated polyacrilyc acid is reached, providing a high degree of particle stabilization for suspensions in a wide range of solids loading. These suspensions do not exhibit any detectable time dependent rheological properties. Increase in particle concentration leads to transition from pseudoplastic to plastic flow behavior. As shear stress decreases, asymptotic increase in viscosity is observed for suspensions with higher solid volume fractions, starting from $\Phi = 0{\cdot}5$. For describing shear-dependent behavior of these systems, the generalized Casson model gives the best fitting results. The apparent Casson yield stress is found to be the most representative quantity to outline the influence of solid volume fraction on the flow properties. From the variation of apparent yield stress with increasing solid volume fraction, a first qualitative picture of the structural conditions of the disperse phase can be drawn. The addition of polyacrilyc acid as a dispersant produces electrosterical stabilization and only limited steric effects occur due to the adsorbed polymer barrier. Different structural arrangements of the disperse phase, governed by electrostatic particle repulsion, are probably one of the reasons for the strong particle concentration dependence of the relative viscosity which cannot be described satisfactorily by any of the existing models for $\eta_r(\Phi)$.

A more detailed picture of the structural conditions of the disperse phase is obtained by examination of viscoelastic properties of studied suspensions. This means that under non-destructive conditions of small amplitude oscillations, the viscous and elastic contributions of viscoelastic

response are more sensitive to microstructural changes with increasing solid concentration. The upper limit of the linear viscoelastic regime (LVR), determined from strain sweep experiments, ranges from 1 to 5% of the strain amplitude. The analysis of viscoelastic data within LVR starts from the application of the Friedrich–Brown model, which belongs to the class of fractional derivative models. The variations of the model parameters with increasing solid volume fraction clearly indicate two critical conditions, related to microstructural changes occurring at Φ values around 0·50 and 0·55. Within this narrow Φ range, transition of viscoelastic behavior from more viscous to more elastic takes place. At the upper limit ($\Phi = 0{\cdot}55$) the viscoelastic response passes from sol-like to gel-like behavior. In order to check the validity of this observation, the analysis of viscoelastic data is extended to a more conventional approach by using the generalized Maxwell model. From the variation of spectrum coefficients another type of particle arrangements can be expected for suspensions at $\Phi \leq 0{\cdot}55$.

Considering the arguments above, the solid volume fractions of 0·5 and 0·55 were selected in order to check the influence of latex binder addition on the rheological behavior of investigated alumina suspensions. When the flow curves of suspensions composed without and with latex binder are compared at the same solid volume fractions, only small differences are observed due to the presence of latex binder More pronounced effects of different disperse phase compositions are detected for the viscoelastic data. Hence, addition of the latex does not seem to cause destabilization of the suspension, but results in an increase in repulsive particle interactions which leads to a tighter particle network structure at rest.

Acknowledgements

This work was performed within the frame of the Human Capital and Mobility Programme (contract no. CHRX CT94 0574) One of the authors (A.Z.) would like to acknowledge the Slovenian Science Foundation for its financial support (grant no. 0092–96).

References

1. Omatete, O., Janney, M. A. and Strehlow, R. A., Gel-casting—a new ceramic forming process. *Am. Ceram. Soc. Bull.*, 1991, **70**(10), 1643–1646.
2. Graule, T. J., Baader, F. H. and Gauckler, L. J. Shaping of ceramic green compacts from suspensions by enzyme catalysed reactions. cfi/Ber. DKG71 (6), 1994.
3. Kosmac, T., Novak, S. and Sajko, M., Net-shaping of ceramic green parts by hydrolysis assisted solidification (HAS). *Fourth Euro Ceramics*, 1995, **1**, 375–382.
4. Adams, R. W, Householder, W. B. and Sundback, B. A., Applicability of quickset injection molding to intelligent processing of ceramics. *Ceram. Eng. Sci. Proc.*, 1991, **12**, 2062–2071.
5. Kristofferrson, A., Roncari, E. and Galassi, C., Aqueous tape casting of alumina with different binders. Submitted to *Journal of the European Ceramic Society*.
6. Greenwood, R. and Bergström, L., Electroacoustic and rheological properties of aqueous Ce–ZrO_2 (Ce–TZP) suspensions. *Journal of the European Ceramic Society*, in press.
7. Braun, L., Morris, J. R. and Cannon, W. R., Viscosity of tape-casting slips. *Am. Ceram. Soc. Bull.*, 1985, **64**(5), 727–729.
8. Cesarano III, J., Aksay, I. A. and Bleier, A., Stability of aqueous α-Al_2O_3 suspensions with poly(methacrylic acid) polyelectrolyte. *J. Am. Ceram. Soc.*, 1988, **71**(4), 50–55.
9. Cesarano III, J. and Aksay, I. A., Processing of highly concentrated aqueous α-alumina suspensions stabilized with polyelectrolytes. *J. Am. Ceram. Soc.*, 1988, **71**(12), 1062–1067.
10. Barnes, H. A., The yield stress myth. In *Proceedings of the XIth International Congress on Rheology*, Brussels, ed. P. Moldenares and R. Keunings. Elsevier Science, Amsterdam, 1992, pp. 576–578.
11. Wildemuth, C. R. and Williams, M. C., Viscosity of suspensions modeled with a shear-dependent maximum packing fraction. *Rheol. Acta.*, 1984, **23**, 627–635.
12. Lapasin, R., Grassi, M. and Pricl, S., Rheological modelling of fractal and sense suspensions. *Chem. Eng. J.*, 1996, **64**, 99–106.
13. Pugh, R. J. and Bergström, L. (eds), Rheology of concentrated suspensions, in *Surface and Colloid Chemistry in Advanced Ceramics Processing*, Surfactant Science Series Vol. 51. Marcel Dekker, New York, 1994, pp. 193–244.
14. Dobiàš, B. (ed.), Structure formation in Disperse systems, in *Coagulation and Flocculation, Theory and Applications*, Surfactant Science Series, Vol 47. Marcel Dekker, New York, 1993, pp. 284–288.
15. Zupancic, A., Lapasin, R. and Zumer, M., Rheological characterisation of shear thickening TiO_2 suspensions in low molecular polymer solution. *Prog. Org. Coat.*, 1997, **30**, 67–78.
16. Winter, H. H. and Chambon, F., Analysis of linear viscoelasticity of a crosslinking polymer at the gel point. *J. Rheol.*, 1986, **30**, 367–382.
17. Chambon, F. and Winter, H. H., Linear viscoelasticity at the gel point of a crosslinking PDMS with unbalanced stoichometry. *J. Rheol.*, 1987, **31**, 683–697.
18. Friedrich, Chr. and Braun, H., Generalized Cole–Cole behavior and its rheological relevance. *Rheol. Acta*, 1992, **31**, 309–322.